PNAS RESEARCH ARTICLE | NEUROSCIENCE

Distinct lateral hypothalamic CaMKIIα neuronal populations regulate wakefulness and locomotor activity

Jaime E. Heiss[a], Peng Zhong[a,1], Stephanie M. Lee[a], Akihiro Yamanaka[b], and Thomas S. Kilduff[a,2,3]

Edited by Joseph Takahashi, The University of Texas Southwestern Medical Center, Dallas, TX; received September 19, 2023; accepted March 14, 2024

For nearly a century, evidence has accumulated indicating that the lateral hypothalamus (LH) contains neurons essential to sustain wakefulness. While lesion or inactivation of LH neurons produces a profound increase in sleep, stimulation of inhibitory LH neurons promotes wakefulness. To date, the primary wake-promoting cells that have been identified in the LH are the hypocretin/orexin (Hcrt) neurons, yet these neurons have little impact on total sleep or wake duration across the 24-h period. Recently, we and others have identified other LH populations that increase wakefulness. In the present study, we conducted microendoscopic calcium imaging in the LH concomitant with EEG and locomotor activity (LMA) recordings and found that a subset of LH neurons that express Ca^{2+}/calmodulin-dependent protein kinase IIα (CaMKIIα) are preferentially active during wakefulness. Chemogenetic activation of these neurons induced sustained wakefulness and greatly increased LMA even in the absence of Hcrt signaling. Few LH CaMKIIα-expressing neurons are hypocretinergic or histaminergic while a small but significant proportion are GABAergic. Ablation of LH inhibitory neurons followed by activation of the remaining LH CaMKIIα neurons induced similar levels of wakefulness but blunted the LMA increase. Ablated animals showed no significant changes in sleep architecture but both spontaneous LMA and high theta (8 to 10 Hz) power during wakefulness were reduced. Together, these findings indicate the existence of two subpopulations of LH CaMKIIα neurons: an inhibitory population that promotes locomotion without affecting sleep architecture and an excitatory population that promotes prolonged wakefulness even in the absence of Hcrt signaling.

sleep | activity | hypothalamus | glutamatergic | electroencephalogram

Significance

Although the lateral hypothalamus (LH) is well-known to contain neurons essential to sustain wakefulness, the primary wake-promoting cells identified to date in this brain region are the hypocretin/orexin (Hcrt) neurons. Here, we show that LH Ca^{2+}/calmodulin-dependent protein kinase IIα (CaMKIIα)-expressing neurons are active during wakefulness and that chemogenetic excitation of these neurons induces sustained wakefulness and increased locomotor activity even in the absence of Hcrt signaling. Ablation of inhibitory LH neurons revealed two CaMKIIα neurons subpopulations: an inhibitory population that promotes locomotion and an excitatory population that prolongs wakefulness. These results advance our understanding of the circuits that regulate sleep/wake and may lead to the development of new therapies to treat sleep/wake disorders such as narcolepsy.

The hypothalamus is among the most phylogenetically conserved regions in the vertebrate brain, reflecting its critical role in maintaining physiological and behavioral homeostasis. By integrating signals arising from both the brain and periphery, it governs a litany of behaviorally important functions essential for survival (1). The hypothalamus contains a diversity of neurons; at least 62 different neuronal subtypes (half of them glutamatergic) have been identified to date (2–4). Distinct cell types in the lateral hypothalamic area (LH) are central to the orchestration of sleep–wake states, feeding, energy balance, and social and motivated behaviors (1, 5–7). Optogenetic manipulation of some of these subpopulations has demonstrated their involvement in different aspects of arousal, feeding, and the stress response. In particular, hypocretin/orexin (Hcrt), melanin-concentrating hormone (MCH), and GABAergic cells in LH have been shown to participate in the regulation of arousal (8, 9).

For nearly a century, the LH has been thought to play a critical role in sleep–wake regulation (10). Lesions and acute inhibition of LH neurons are known to increase sleep time (11–15) while excitation produces arousal and increased activity (16–19). Several studies have identified wake-active neurons in the LH (20–22) but their neurochemical identity and specific physiological roles are unclear. Hcrt neurons have been the most extensively studied wake-promoting LH neuronal population to date (9, 23–29). These cells project to several wake-promoting areas of the brain including the basal forebrain (BF), the tuberomamillary nucleus (TMN), and the locus coeruleus (LC) where they can release the Hcrt peptides, glutamate, dynorphin, and perhaps other neurotransmitters (26–29). In this regard, the Hcrt neurons have been proposed to act like a stabilizer of a flip-flop switch that controls behavioral state (30).

Recently, optogenetic and chemogenetic studies have identified other LH neuronal populations that induce or prolong wakefulness including GABAergic cells (31, 32), peptidergic neurons (33), and *Vglut2*-expressing cells (34). Chemogenetic stimulation of LH glutamatergic neurons resulted in an impressive increase in wakefulness that persisted for 6 h (35), strongly resembling results that we described previously (36) and found to be independent of the LH populations known to be involved in locomotor activity (LMA) (37–40). Since glutamatergic neurons are widespread within the LH as well as throughout

Author contributions: J.E.H., P.Z., S.M.L., and T.S.K. designed research; J.E.H., P.Z., and S.M.L. performed research; A.Y. contributed new reagents/analytic tools; J.E.H., P.Z., and T.S.K. analyzed data; and J.E.H., P.Z., and T.S.K. wrote the paper.

The authors declare no competing interest.

This article is a PNAS Direct Submission.

[1]Present address: Department of Neurological Sciences, College of Medicine, University of Nebraska Medical Center, Omaha, NE 68198.

[2]Present address: Chinese Institute for Brain Research (CIBR), Beijing 102206, China.

[3]To whom correspondence may be addressed. Email: thomas.kilduff@sri.com.

This article contains supporting information online at https://www.pnas.org/lookup/suppl/doi:10.1073/pnas.2316150121/-/DCSupplemental.

Published April 9, 2024.

the nervous system, a more specific neurochemical marker of these LH wake-promoting systems is desirable to facilitate further studies.

The sleep disorder Narcolepsy is widely accepted to be due to the extensive loss of Hcrt neurons (41–43). Although sodium salt of gamma-hydroxybutyrate (GHB) is an effective therapeutic for the treatment of narcolepsy symptomatology, the biochemical and neurobiological basis of its therapeutic efficacy is unknown (44). However, GHB has recently been shown to bind selectively to the hub region of calcium/calmodulin-dependent protein kinase IIα (CaMKIIα). CaMKIIα expression is commonly used as a marker for excitatory pyramidal neurons in the cortex and exhibits little overlap with GABAergic cells (45, 46), except in a few areas such as the granule cells in the olfactory bulb, cerebellar Purkinje cells, and some neocortical layer I cells (47). Since CaMKIIα-expressing neurons are primarily glutamatergic and LH glutamatergic cells are wake-promoting, we investigated whether CaMKIIα might be a more specific marker of the LH wake-promoting population. We find that LH CaMKIIα neurons are wake-active and that chemogenetic excitation of LH CaMKIIα cells induces sustained wakefulness and increased LMA even in the absence of Hcrt signaling. Since local ablation of LH GABAergic cells reduced LMA but did not affect either spontaneous or CaMKIIα neuron-stimulated sleep/wake amounts, we suggest that only the glutamatergic LH population participates in regulation of sleep and wake whereas the GABAergic population affects LMA. These insights into LH wake-promoting neuronal populations could lead to identification of a unique therapeutic pathway for the treatment of disorders of excessive sleepiness such as hypersomnia and narcolepsy.

Results

Chemogenetic Activation of LH Glutamatergic Neurons Promotes Sustained Wakefulness. As a first step, we sought to verify that activation of LH glutamatergic neurons promoted wakefulness as described by Wang and colleagues (35). Accordingly, we injected 8 *Vglut2-IRES-Cre* mice with 100 nL of AAV8-hSyn-DIO-hM3D(Gq)-mCherry into the LH at −1.4 mm AP, ±1.2 mm ML, −5.0 mm DV (from bregma). The transfection occupied most of the area lateral to fornix and medial to the cerebral peduncle (*SI Appendix*, Fig. S1*E*). To test whether the activation of these cells elicited wakefulness, we injected either saline (SAL) or the hM3Dq agonist deschloroclozapine (DCZ; Hello bio #HB8555; 0.3 mg/kg, i.p.) (48, 49) at ZT2 in a repeated measures design in which all mice received both treatments at least 1 wk apart. DCZ-mediated activation of LH *Vglut2* neurons evoked nearly continuous Wake for 6 h at a time of day when sleep pressure is very high (*SI Appendix*, Fig. S1*A*). As we showed previously for clozapine-N-oxide (CNO) when tested at the specific dose used at this particular time of day (36), DCZ had no significant effect on naive mice. Two-way repeated measures ANOVA (RM-ANOVA) confirmed a significant interaction between treatment and time ($F_{(11,77)} = 9.88$, $P < 0.001$, $n = 8$, two-way RM-ANOVA followed by Bonferroni post hoc *t* test).

Spectral analysis of the EEG during Wake revealed a significant interaction between treatment and the different EEG power spectral bands ($F_{(5,35)} = 7.32$, $P < 0.001$, $n = 8$, two-way RM-ANOVA; *SI Appendix*, Fig. S1 *C* and *D*). The EEG frequencies were grouped into the following bands: delta (δ), 0.5 to 4 Hz; low theta (Lθ), 4 to 8 Hz; high theta (Hθ), 8 to 10 Hz; low gamma (Lγ), 15 to 50 Hz; high gamma (Hγ), 60 to 80 Hz; and very high gamma (Vhγ), 90 to 200 Hz. Bonferroni-corrected *post hoc t* tests indicated that the normalized power during Wake for the Hθ (8 to 10 Hz) and Hγ (60 to 80 Hz) bands after DCZ treatment was significantly increased to 145% and 180%, respectively, of their values after SAL treatment (*SI Appendix*, Fig. S1*D*). The increase of high θ power during wake (HθWP) upon activation of LH *Vglut2* neurons persisted for several hours (*SI Appendix*, Fig. S1*B*) with a significant treatment x time interaction after dosing ($F_{(11,77)} = 3.87$, $P < 0.001$, $n = 8$, two-way RM-ANOVA followed by Bonferroni-corrected post hoc *t* tests). HθWP has been identified as an electrophysiological marker of behavioral locomotion and exploration (50–52). In conjunction with elevated EMG levels, these results suggested that the wake-promoting effects observed after excitation of LH *Vglut2* neurons involve increased LMA and are produced by glutamatergic neurons located between the fornix and the optic tract.

Chemogenetic Activation of LH CaMKIIα-expressing Neurons Promotes Sustained Wakefulness in the Absence of Hcrt Signaling. To determine whether the wake promotion that we (36) and others (35) described previously (and which is replicated in *SI Appendix*, Fig. S1) could be mediated by LH CaMKIIα-expressing neurons and whether Hcrt signaling was involved, we injected 370 nL of AAV8-CaMKIIα-HA-hM3D(Gq)-IRES-mCitrine bilaterally into the LH (−1.4 mm AP, ±1 mm ML, −4.8 mm DV from pia) of male C57BL6/J (WT) mice (8 to 12 wk of age). We have previously shown that reducing Hcrt neurotransmission with the dual Hcrt receptor antagonist almorexant (ALM) at doses of 100 to 300 mg/kg, i.p., significantly increased nonrapid eye movement sleep (NREM) sleep and decreased Wake in WT mice (36, 53). After recovery from surgery and acclimation to dosing and tethers, mice received either ALM (200 mg/kg, i.p.) or vehicle (HPMC) at ZT4 and, one hour later, either the hM3Dq agonist CNO (3 mg/kg, i.p.) or SAL while the EEG and EMG were recorded continuously from ZT3 to ZT12. All mice received all treatment pairings; at least 1 wk elapsed after CNO treatment. Although CNO at this concentration can present off target effects (54), we have previously shown that this CNO concentration did not affect wakefulness in WT mice at this time of day (36).

Fig. 1*A* illustrates that, while the combination of ALM at ZT4 followed by SAL at ZT5 (green line) transiently reduced the amount of Wakefulness in comparison to the VEH–SAL combination (black line) at a time of day when sleep levels are high (in particular, during ZT5 and ZT9, where the X at the top of the graph indicates a significant hourly difference), activation of CaMKIIα-hM3Dq-transfected LH neurons (magenta line) produced a strong wake-promoting effect even in the presence of the Hcrt receptor antagonist ALM (blue line). LH CaMKIIα neuron activation increased wakefulness for 7 h post-CNO injection (magenta and blue vs. black and green lines); a significant treatment × time interaction was found for the percent time spent in Wake during the post-dosing period (ZT5-ZT12; $F_{(24,72)} = 17.53$, $P < 0.001$, $n = 4$, two-way RM-ANOVA). There were no differences between the ALM-CNO (blue) and VEH-CNO (magenta) treatments for any state during this period, indicating that blockade of Hcrt neurotransmission had no effect on the hourly amounts of wakefulness produced by activation of LH CaMKIIα neurons despite the fact that ALM is known to induce sleep at even lower doses (36, 53).

Fig. 1*B* presents the percentage of time spent in Wake bouts of different durations for the first 5 h after dosing (ZT5-10) for the four dosing conditions. Not surprisingly, the ALM–SAL combination (green line) suppressed longer Wake bouts compared to the VEH–SAL combination (black line) as most of the time awake was spent in Wake bouts shorter than 2 min. Conversely, the overall Wake bout distribution was shifted toward

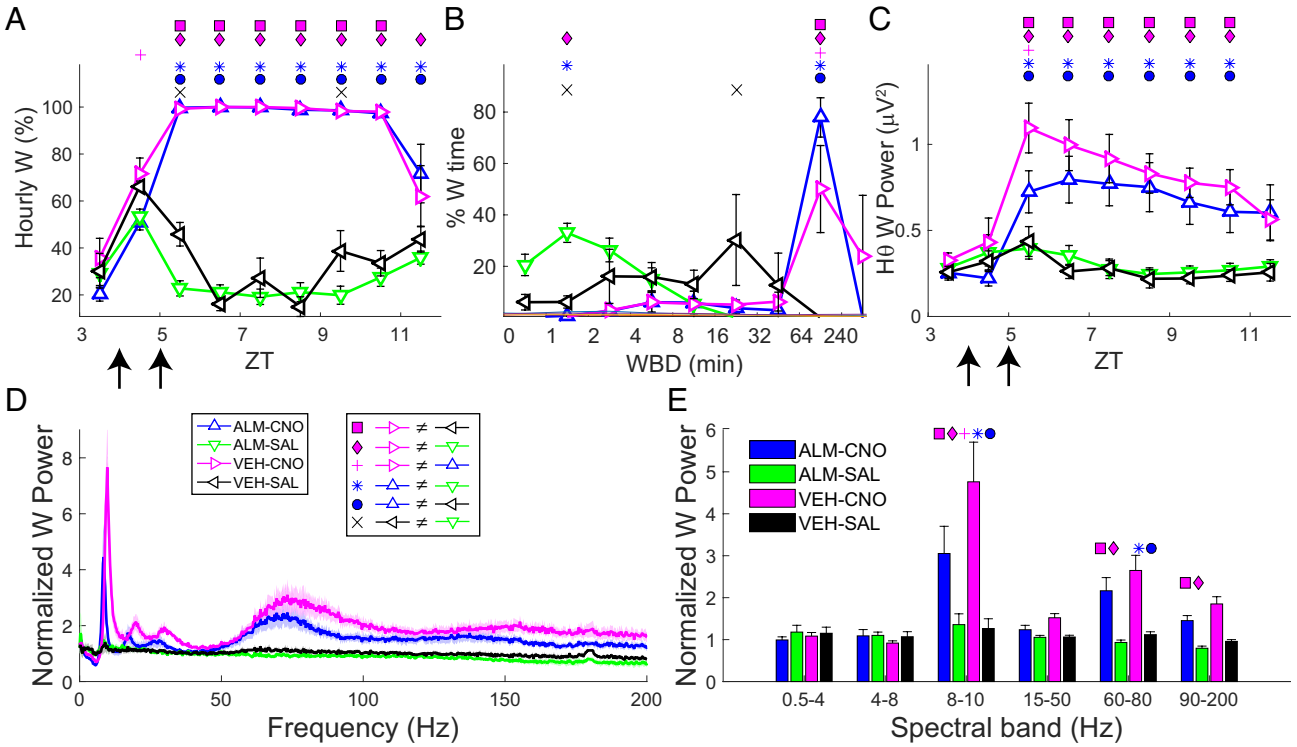

Fig. 1. Chemogenetic activation of LH CaMKIIα neurons in C57BL6/J mice induces prolonged wakefulness independent of Hcrt neurotransmission. (*A*) Hourly percentage of time spent in Wake (W) in C57BL6/J mice after i.p. injection of either VEH or ALM at ZT4 followed by either SAL or CNO at ZT5. Arrows at the *Bottom Left* of the abscissa indicate the times of dosing. Symbols above each time point denote significant hourly differences between the indicated treatments according to the legends in panel *D*. (*B*) Time-weighted frequency histograms showing the proportion of wake bout durations from ZT5 to ZT10 collapsed into different duration bins, relative to the total amount of wakefulness from ZT5 to ZT10 for the different experimental treatments. (*C*) Time course of high θ power (8 to 10 Hz) during W for the four experimental treatments. (*D*) Normalized EEG power spectrum (0 to 200 Hz) during wakefulness (W) from ZT5 to ZT8 for the different experimental treatments. (*E*) Mean power in the EEG spectral bands after treatment (ZT5 to ZT8), normalized to baseline. Symbols above the data denote significant differences for the comparisons indicated in the legends in panel *D* ($P < 0.05$, $n = 4$, two-way RM-ANOVA followed by Bonferroni post hoc *t* test).

longer Wake bouts for the VEH–CNO (magenta line) and ALM–CNO (blue line) treatments; most of the Wake time was spent in >64 min long bouts. Significantly more Wake time was spent in 64 to 240 min bin after ALM–CNO than after VEH–CNO ($P < 0.05$, $n = 4$, Bonferroni post hoc *t* test), as the VEH–CNO combination resulted in several Wake bouts longer than 240 min, indicating that Hcrt receptor blockade in the ALM–CNO combination prevented the occurrence of Wake bouts longer than 4 h. Due to the absence of sleep bouts in most mice after CNO injection, no statistical analyses were performed on sleep bout durations.

As described above for LH *Vglut2* neurons, activation of LH CaMKIIα-hM3Dq-transfected neurons induced a large increase in the EEG power spectrum, especially in HθWP and >60 Hz ranges (Fig. 1 *C*–*E*). A strong treatment x time interaction was observed for HθWP after dosing ($F_{(24,72)} = 5.38$, $P < 0.001$, $n = 4$, two-way RM-ANOVA). *Post hoc* analysis revealed that HθWP after the VEH–CNO treatment (magenta) was significantly higher than the other three treatments during ZT5-6 (Fig. 1*C*) and that, as depicted by the symbols above the respective ZT intervals in Fig. 1*C*, both CNO-treated groups had significantly higher HθWP than SAL-treated subjects for 6 h after dosing, even in the presence of ALM (blue line). Two-way RM-ANOVA revealed a significant treatment x power band interaction ($F_{(15,45)} = 18.03$, $P < 0.001$, $n = 4$), as illustrated in Fig. 1*E* in which the symbols above the bars denote significant differences between pairs of conditions. The normalized power for the VEH-CNO treatment (magenta) for the Hθ, Hγ, and Vhγ bands was 377%, 237%, and 193% of their respective values after VEH-SAL treatment.

CaMKIIα-expressing Neurons in the LH Are Wake-active. Since chemogenetic activation of LH CaMKIIα-hM3Dq-transfected neurons produced sustained Wake bouts, we sought to determine the endogenous activity of LH CaMKIIα cells across the sleep–wake cycle using microendoscopic Ca^{2+} imaging. Under isoflurane anesthesia, adult male (n = 2) and female (n = 2) C57BL6/J wild-type (WT) mice were injected in the LH (–1.4 mm AP, –1.2 mm ML, –4.7 mm DV from pia) with 370 nL of an AAV encoding the calcium indicator GCaMP6f (AAV9-CamKII-GCaMP6f-WPRE) (55). After a 2 wk incubation period, mice were implanted with skull screws for EEG recording, EMG electrodes in the nuchal musculature and a 0.5-mm diameter gradient refractive index (GRIN) lens was placed over the LH. At least 2 wk after lens and EEG/EMG electrode implantation, imaging was performed in freely-moving mice through the GRIN lens coupled to a miniaturized integrated fluorescence microscope (56).

Fig. 2*A* shows a representative recording of the Ca^{2+} dynamics of 3 CaMKIIα-expressing neurons monitored across a ~2 h recording session, as well as the corresponding hypnogram which depicts the progression of arousal states in 4-sec epochs during the recording. In this example, the color of the traces represents the Z-scores of the Ca^{2+} dynamics (i.e., relative activity) during Wake (green), NREM sleep (blue), and rapid eye movement (REM) sleep (red). Fig. 2*B* shows the relative location of the 56 CaMKIIα neurons recorded in the LH of this mouse; the neurons are color-coded to indicate their state "preference" according to the color scheme in the triangle. The predominance of green with little red or blue denotes the skew toward greater activity during Wake for the vast majority of the CaMKIIα neurons recorded. In ~29% of LH CaMKIIα neurons, the mean Z score was significantly greater

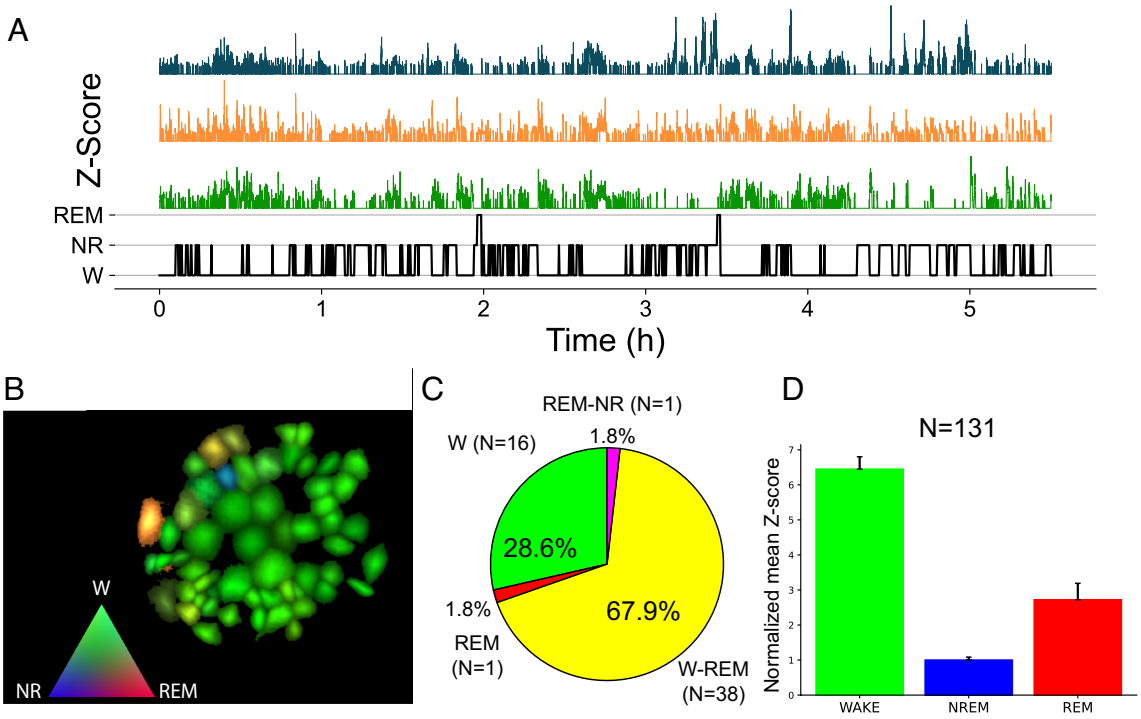

Fig. 2. Ca^{2+} dynamics of LH CaMKIIα neurons across arousal states in C57BL6/J mice injected with 370 nL of AAV9-CaMKII-GCaMP6f-WPRE. (*A*) Concatenated Ca^{2+} traces from three LH CaMKIIα neurons color-coded according to the triangle legend in *B* to reflect the behavioral state "preference" of these cells. The hypnogram at the *Bottom* of panel *A* shows the sequence of behavioral states across the recording period. (*B*) LH CaMKIIα neurons identified as sources of independent changes in fluorescence (overlap of the normalized maximum $\Delta F/F_0$ of 56 cells). Cells were colored according to the triangle to indicate their behavioral state preference where the amount of red (REM), green (wake), and blue (NREM) represents the weighted sum of the Z-score for each state, normalized for each neuron. Thus, for example, the left-most orange cell and corresponding trace had twice the average Z-score during REM than during W and a very low Z score during NREM. (*C*) Behavioral state preference ($P < 0.05$) of a mouse in which 56 LH CaMKIIα cells were classified by state preference as mixed W and REM sleep preference ($n = 38$ cells), only W ($n = 16$ cells), only REM ($n = 1$ cell), and mixed REM-NREM preference ($n = 1$ cell). (*D*) Population average showing mean Z-score across states relative to the Z-score during NREM sleep for 131 cells recorded in four mice. Asterisks denote significant difference ($P < 0.05$) between states after Bonferroni correction.

during Wake than during NREM or REM sleep (Fig. 2*C*). All but two of the remaining cells showed a significantly greater response during Wake and REM than during NREM. There were too few epochs of REM sleep to derive a meaningful conclusion about the behavioral state preference of neurons during this state (three of the four mice didn't show any REM epochs during the 120-min recordings). The durations of the recording sessions were limited by the technical capabilities of in vivo microendoscopic recordings concomitant with EEG/EMG tether recordings (e.g., implant weight, cell registration after prolonged periods). The mean (±SEM) Z-scores across all mice, each normalized to its mean Z-score during NREM, were 6.45 ± 0.35 for Wake, 2.72 ± 0.77 for REM, and 1.00 ± 0.09 for NREM (Fig. 2*D*), all significantly different from each other (Bonferroni *t* test, $P < 0.05$; W: $n = 131$, NREM: $n = 131$, REM: $n = 56$). These results indicate that LH CaMKIIα neurons are predominantly Wake-active with, on average, more than a sixfold increase in Z-score during Wake compared to NREM sleep.

Most CaMKIIα-expressing Neurons in the LH Are neither Hypocretinergic, Histaminergic, nor GABAergic. To evaluate whether CaMKIIα-hM3Dq was expressed in the currently known LH wake-promoting neuronal populations, we performed double-labeled immunohistochemistry on mice that had received bilateral LH injections of AAV8-CaMKIIα-HA-hM3D(Gq)-IRES-mCitrine (Fig. 1) to assess the expression of hM3Dq in LH Hcrt and histaminergic neurons and used a similar preparation to verify expression of hM3Dq in LH GABAergic cells. Mice were perfused transcardially with 4% paraformaldehyde and the brains were sectioned into 30-µm coronal slices. After immunostaining for Hcrt, we identified on average 987 ± 88 Hcrt neurons per mouse ($n = 3,949$ Hcrt cells in total) and found that 9.3 ± 0.5% of these cells were transfected with hM3Dq ($n = 363$ cells). Despite the high density of hM3Dq-mCitrine-transfected neurons in the LH region in which the Hcrt cells are located, the white arrows indicating the position of Hcrt cells in Fig. 3*A* illustrate the relative absence of overlap of these two populations.

To determine whether histaminergic neurons were transfected with hM3Dq, we used a rabbit anti-adenosine deaminase (ADA) antibody and donkey anti-rabbit Alexa Fluor 568 and counted the number of labeled cells. Fig. 3*B* shows microphotographs of histaminergic cells (left) and hM3Dq-mCitrine-transfected neurons (right). The white arrows in both panels indicate the location of histaminergic cells and the pink arrows identify two double-labeled neurons. We found on average 95 ± 27 histaminergic cells per mouse ($n = 378$ cells in total) and that only 6 ± 3% ($n = 25$ cells) were transfected with hM3Dq.

To determine whether CaMKIIα-dependent hM3Dq was expressed in LH inhibitory as well as excitatory neurons, we injected bilaterally 100 nL of AAV8-CaMKIIα-hM3D(Gq)-mCherry in 3 *Gad2*-IRES-Cre;*R26R-EYFP* mice to identify the percentage of transfected neurons that correspond to inhibitory neurons. This mouse reporter has been shown to label almost all inhibitory neurons with >90% of both specificity and efficiency (57). Using a chicken anti-GFP antibody and donkey anti-chicken Alexa Fluor 488 to identify inhibitory neurons together with rabbit anti-red fluorescent protein (RFP) antibody and donkey anti-rabbit Alexa Fluor 568, we counted RFP-labeled cells around each bilateral injection site in four to five slices per mouse ($n = 2,486$ transfected cells)

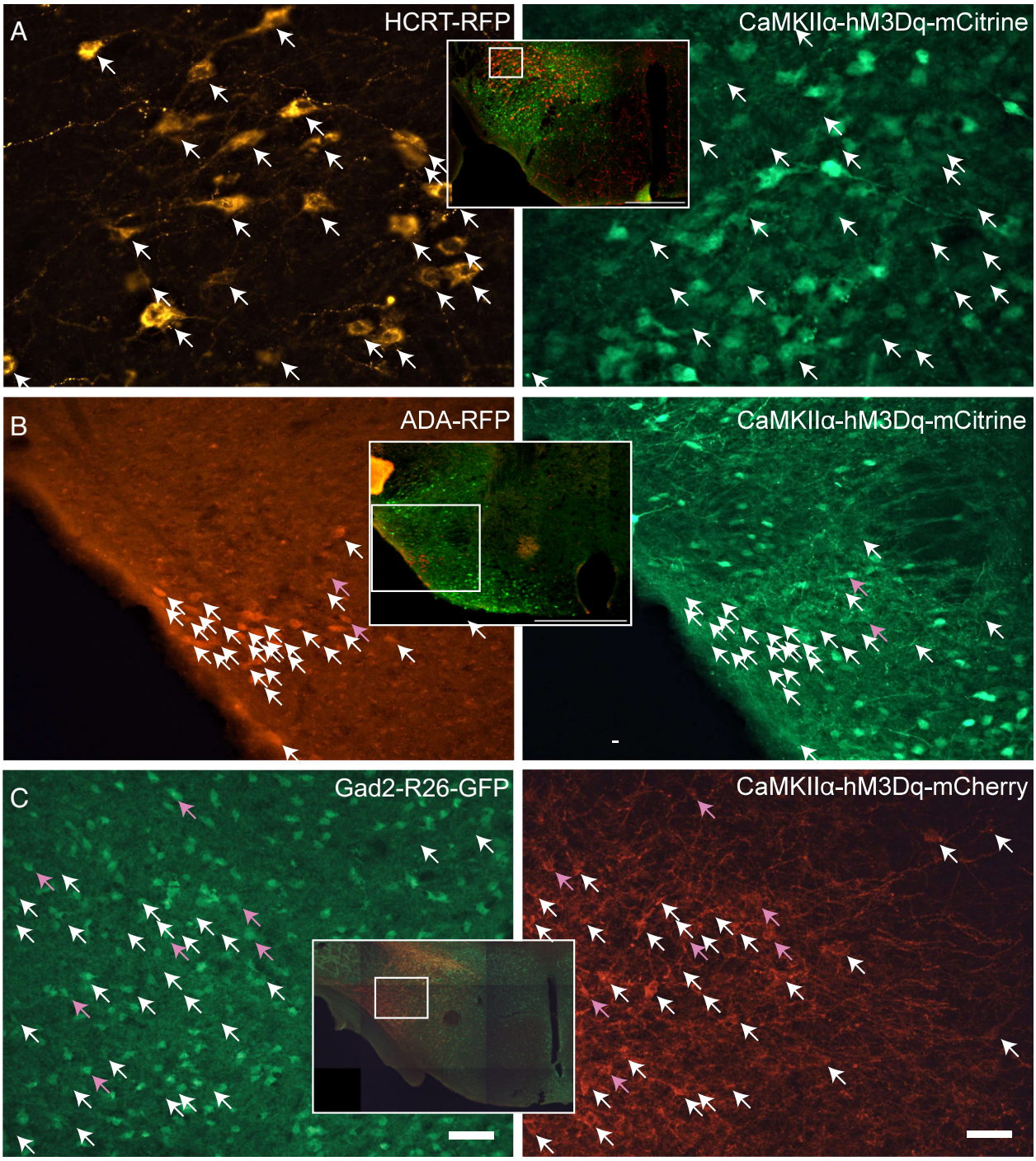

Fig. 3. Transfected CaMKIIα-hM3Dq neurons in C57BL6/J mice have limited overlap with currently known W-promoting neurons. (*A*) Photomicrographs showing Hcrt neurons (*Left*) and CaMKIIα-hM3Dq-citrine neurons (*Right*). White arrows indicate the absence of overlap between the two populations. (*B*) Photomicrographs showing ADA$^+$ neurons (*Left*) and CaMKIIα-hM3Dq-Citrine transfected neurons (*Right*) in the tuberomammillary nucleus. Two neurons are double-labeled (pink arrows), whereas the majority of ADA$^+$ neurons are single-labeled (white arrows). (*C*) Inhibitory neurons identified in *Gad2-IRES-Cre;R26R-EYFP* mice after injection with AAV8-CaMKIIα-hM3Dq-mCherry (*Right*) showing seven double-labeled cells (pink arrows) among 27 single-labeled inhibitory neurons (white arrows). (Scale bar in *C*: 25 μm for *A*, 100 μm for *B* and 50 μm for *C*.) All images are coronal sections. The white boxes within the insets show lower magnification merged pictures of similar imaged areas. Scale bar of *Insets* in *A* and *B* corresponds to 500 μm.

and then determined how many of them were also GFP-labeled cells. We found that 20.1 ± 0.7% of RFP-labeled cells were also Gad2+ neurons, indicating that a minority but a significant percentage of LH CaMKIIα neurons are inhibitory cells. Fig. 3*C* presents microphotographs of GABAergic cells (left) and hM3Dq-mCherry-transfected neurons (right) showing seven double-labeled neurons indicated by pink arrows whereas single-labeled hM3Dq-transfected neurons are indicated by white arrows.

To address the possibility that the AAV8-CaMKIIα-HA-hM3D(Gq)-IRES-mCitrine and AAV9-CamKIIα-GCaMP6f-WPRE constructs that we used targeted non-CaMKIIα-expressing cells in the LH, we conducted a fluorescent in situ hybridization study in which we counted 934 mCherry-labeled cells from 3 mice and found that 95.6 ± 0.4% coexpressed CaMKIIα (*SI Appendix*, Fig. S2, *Top* row). Furthermore, we identified two subpopulations of CaMKIIα neurons: one in which 78.7 ± 3.7% of 708 mCherry-labeled

neurons coexpressed *Vglut2* (*SI Appendix*, Fig. S2, *Middle* row) and another in which 33 ± 2.2% of 613 mCherry-labeled neurons expressed *Vgat* (*SI Appendix*, Fig. S2, *Bottom* row). These proportions were similar to that described above using immunohistochemistry of the *Gad2* promoter as a proxy for *Vgat* and assuming the absence of *Gad2* as a proxy for *Vglut2*.

LH GABAergic Neurons Are Not Part of the Arousal Circuit but Are Necessary for CNO-induced Hyperactivity. Chemogenetic stimulation of some LH GABAergic neurons can produce arousal (31), while Hcrt neurons as well as LH GABAergic neurons directly regulate LMA (37–40). Although there is little overlap between inhibitory and CaMKIIα-expressing neurons in most cortical regions, this is not necessarily the case in other brain areas (47) as shown in Fig. 3*C*. Inhibitory neurons may also be a downstream target of excitatory CaMKIIα neurons or a subset of GABAergic LH CaMKIIα neurons could directly mediate the Wake-promoting effects shown in Fig. 1. To determine whether GABAergic neurons are necessary for the arousal triggered by LH CaMKIIα neuron activation, we coinjected 100 nL of a 50 to 50 mixture of AAV8-CaMKIIα-hM3D(Gq)-mCherry and AAV-CMV-FLEX-mCherry/DTA (Sr10) into the LH (–1.4 mm AP, –1.2 mm ML, –4.7 mm DV from pia) of *Gad2-IRES-Cre;R26R-EYFP* (TG; n = 10) mice and WT (n = 9) littermates. Although this strategy resulted in expression of hM3Dq in LH CaMKIIα neurons in both mouse strains, the GABAergic neurons around the AAV-CMV-FLEX-mCherry/DTA injection site should be ablated by expression of Diphtheria Toxin A (DTA) in the Cre-expressing TG mice but not in the WT mice. This strategy reduced the density of inhibitory cells around the injection site by 64.6%, from a mean density of 800 cells/mm^2 to 285.35 cells/mm^2 (*SI Appendix*, Fig. S3).

At least 8 wk subsequent to the AAV coinjections, mice of both genotypes were administered either CNO (3 mg/kg, i.p.) or SAL at ZT5 while EEG/EMG was recorded from ZT4–ZT12. Bonferroni-corrected t tests showed that CNO treatment elicited similar amounts of wakefulness in both TG (blue line) and WT (green line) mice (Fig. 4*A*), with no significant differences in percentage of Wake time for any hour. Therefore, ablation of LH inhibitory GABAergic neurons did not affect the wake-promoting effects of LH CaMKIIα neuron activation. However, Fig. 4 *B–D* show that there was a strong effect of genotype on EEG power after CNO treatment which was evident when HθWP, the electrophysiological marker for behavioral locomotion and exploration(50–52), was quantified: Ablation of inhibitory neurons in TG mice (blue trace) eliminated the increase in both Hθ and Hγ that occurred in WT mice after CNO treatment (green trace).

We previously showed that, after LH activation, mice exhibited behavior similar to spontaneous wake active periods (36). To determine whether ablation of LH inhibitory cells concomitant with activation of LH CaMKIIα neurons affected waking activity, we computed the LMA speed for both genotypes of mice using a video tracking system (Vium, Inc., San Mateo, CA). At least 6 wk subsequent to AAV injection, mice were dosed with either CNO or SAL at ZT5 and the mean LMA speed from ZT5-ZT10 was compared between treatments and genotypes. In WT mice, CNO

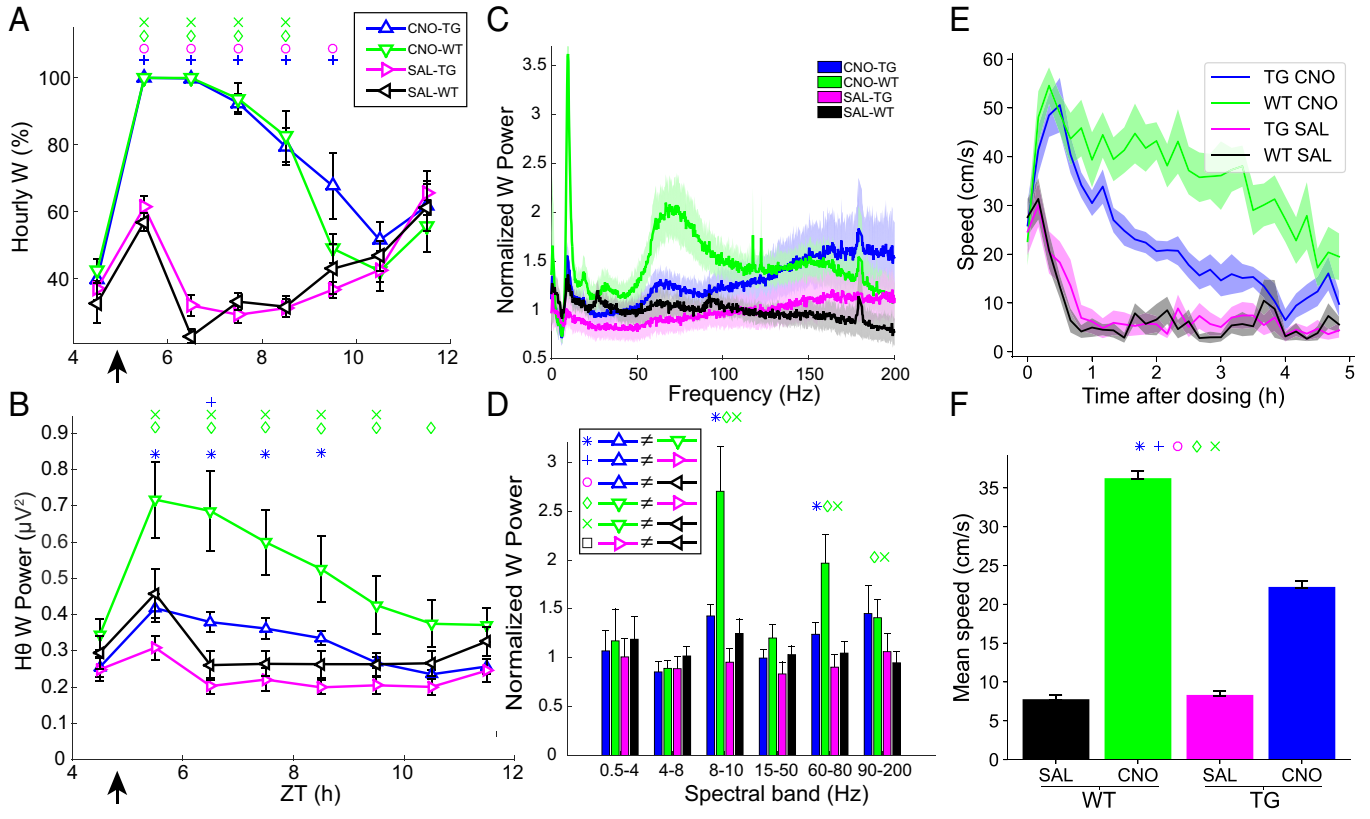

Fig. 4. Ablation of LH inhibitory neurons in TG mice affects LMA but not CaMKIIα neuron-mediated wakefulness. (*A*) Hourly percentage of time spent in W after i.p. injection of either clozapine-N-oxide (CNO) or saline (SAL) at ZT5 in *Gad2-IRES-Cre* (TG) and C57BL6/J (WT) mice that had been transfected with AAV8-CaMKIIα-hM3Dq-mCherry and AAV-CMV-FLEX-DTA in the LH. (*B*) High θ power during W (HθWP) after i.p. injection of either CNO or SAL at ZT5 in TG and WT mice as indicated by the legends in *A* and *D*. (*C*) Normalized EEG power spectrum during W from ZT5 to ZT8 after i.p. injection of either CNO or SAL at ZT5 in TG and WT mice. (*D*) Mean normalized power during Wakefulness for EEG spectral bands in TG and WT mice after treatment with CNO or SAL. (*E*) Locomotor speed (mean ± SEM in 10 min bins) in TG and WT mice after CNO or SAL injection at ZT5. (*F*) Mean locomotor speed for the 5 h after injection of either CNO or SAL in the four experimental groups. Arrows at the *Bottom Left* of the abscissa in *A* and *B* indicate the time of dosing at ZT5. Symbols above the data denote significant differences between the indicated treatments (P < 0.05, n = 9 and n = 10 for WT and TG respectively, Bonferroni post hoc t test) according to the legends in panels *A* and *D*.

significantly increased mean LMA speed 470% from 7.7 ± 0.6 cm/s after SAL to 36.2 ± 3.6 cm/s after CNO treatment (Bonferroni paired *t* test, $P = 7.75 \times 10^{-6}$, $n = 9$) while CNO treatment in TG mice significantly increased mean LMA speed 269% from 8.3 ± 0.6 cm/s after SAL to 22.2 ± 2.1 cm/s after CNO (Bonferroni paired *t* test, $P = 1.13 \times 10^{-5}$, $n = 10$). The difference between genotypes in CNO-induced speed was significantly different (Bonferroni unpaired *t* test, $P = 7.98 \times 10^{-4}$, $n = 9, 10$), indicating that GABAergic neuron ablation in TG mice (blue trace) attenuated the CNO-evoked increase in LMA speed evident in WT mice (green trace; Fig. 4 *E* and *F*).

Ablated as well as intact mice exhibited a relatively normal phenotype during spontaneous active periods as well as during CNO-induced hyperactivity as can be verified from the recorded videos of their behavior in the absence of CNO dosing (Movies S1, S3, S5, and S7) and 30 to 120 min after dosing (ZT6-8) (Movies S2, S4, S6, and S8). To further evaluate whether ablation of LH inhibitory cells had any effects on normal mouse behavior, LMA was analyzed for 24 h in undisturbed conditions and compared between WT and TG mice. LMA speed during the active phase was 68% lower in the ablated TG mice compared to the WT mice (unpaired *t* test, $P = 0.047$, $n = 9$ vs. $n = 10$; *SI Appendix*, Fig. S4).

Since LH GABAergic neuron ablation affected LMA and activity plays an important role in the regulation of sleep/wake, we assessed whether LH GABAergic neuron ablation affected the architecture of sleep/wake states. Despite the attenuation of LMA speed documented above, comparison of 24 h of EEG/EMG recordings in WT ($n = 9$) vs. TG mice ($n = 10$) failed to identify any difference in the hourly percentage of time or bout durations for any sleep state between the two genotypes other than confirmation of the reduction in HθWP in TG mice (*SI Appendix*, Fig. S5). These results indicate that LH inhibitory neurons are necessary for the increase in LMA speed observed during active Wake and suggest that LH inhibitory neurons do not contribute to the wake-promoting pathway elicited by LH-CaMKIIα activation.

Discussion

We previously showed that activation of LH neurons can induce arousal independent of the Hcrt neurons (36) and, in the present study, have sought to identify the relevant LH neuronal population. Previous studies have shown that optogenetic or chemogenetic stimulation of LH Hcrt (58, 59) and LH GABAergic neurons (31, 32) can promote wakefulness. More recently, a population of LH glutamatergic neurons was shown to induce prolonged arousal after chemogenetic stimulation (35), an effect that we confirmed here.

Using calcium imaging, chemogenetic manipulations, and genetically targeted cellular ablation, we have identified CaMKIIα as a marker for LH neurons involved in regulating behavioral states. A recent study (60) has shown that the CaMKIIα promoter can drive protein expression in cortical interneurons in which this protein kinase has been found to be absent both by immunolabeling (45, 46) and RNAscope hybridization (61). Since CaMKIIα is expressed in inhibitory cells in the hippocampus as well as the cortex, these results suggest that the CaMKIIα promoter can drive the expression of transgenes in some non-CaMKIIα-expressing cells as well as in CaMKIIα-expressing cells. To address the possibility that the AAV-CaMKIIα constructs that we used targeted non-CaMKIIα-expressing cells, we conducted both immunohistochemical (Fig. 3) and RNAscope hybridization (*SI Appendix*, Fig. S2) studies and found that almost all *hM3Dq-mCherry*-labeled cells (95.6 ± 0.4%) coexpressed *Camk2a* RNA and ~20 to 30% of the cells labeled by the CaMKIIα promoter were GABAergic.

Our results indicate that LH CaMKIIα-expressing neurons are wake-active, that chemogenetic excitation of these neurons can induce sustained wakefulness even in absence of Hcrt signaling, that these wake-active, wake-promoting cells are neither hypocretinergic nor histaminergic, and that they can be divided into two subpopulations: a glutamatergic wake-promoting population encompassing about 80% of these cells and a GABAergic population encompassing the remaining 20%. Finally, our cellular ablation studies showed that the LH CaMKIIα-expressing GABAergic neurons are involved in LMA and the concomitant changes in EEG activity, i.e., increased HθWP, but they are not involved in arousal per se. Although different preparations, this conclusion is further supported by the relatively mild increase in HθWP during activation of purely glutamatergic cells (145% increase; *SI Appendix*, Fig. S1 *B–D*) in contrast to the increase in HθWP observed after activation of LH CaMKIIα neurons (377%; Fig. 1 *C–E*).

Identification of other neurochemical markers of the CaMKIIα inhibitory neurons in the LH would be of great interest. MCH neurons in the LH have long thought to be GABAergic (62, 63); ~98% of MCH cells express *Gad1* and 21% express *Gad2*. However, *Slc32a1,* which encodes the vesicular GABA transporter, was not found in any MCH neurons (64), which raises a question regarding GABA release by MCH neurons. Previous studies have suggested that at least a subset of MCH neurons are glutamatergic (65, 66) and virtually all MCH cells expressed *Slc17a6,* which encodes the vesicular glutamate transporter 2 (vGlut2) (64). Although LH Hcrt neurons are known to be glutamatergic (26) and, accordingly, all Hcrt cells studied expressed *Slc17a6* (64), surprisingly, 56% of Hcrt neurons expressed *Gad1* and 16% expressed *Gad2*. Although this might suggest that a subset of Hcrt neurons could release GABA as well as glutamate, *Vgat* mRNA was only found in 1.5% of Hcrt neurons (64). As illustrated in Fig. 3*A*, since <10% of the Hcrt cells were transfected with hM3Dq, it is unlikely that Hcrt neurotransmission plays a significant role in the profound wake-promoting effects illustrated in Fig. 1, particularly since these effects persist in the presence of Hcrt receptor blockade by ALM. Since at least 15 GABAergic populations have been identified in the LH to date (2), there are a number of candidate cell types to evaluate in future studies.

The present study provides evidence that the parallel arousal pathway which we described previously (36) is likely mediated by the glutamatergic neurons described by Wang and colleagues (35), which partially overlaps with the CaMKIIα population. The absence of changes in sleep architecture after LH GABAergic cell ablation despite a decrease in LMA contradicts the suggestion of a wake-promoting population of inhibitory neurons in this region (31). One possible explanation is that, although the *Gad2-IRES-Cre* mice express Cre in >90% of inhibitory neurons (57), the wake-promoting inhibitory neurons described by Venner et al. are part of the 10% not represented and that these cells are CaMKIIα negative. Another possibility is that the volume of tissue transfected by our FLEX-DTA AAV injection did not overlap completely with the previously reported GABAergic population and, since the ablation was not 100% effective, the subset of inhibitory neurons not ablated by DTA was sufficient to maintain the sleep regulatory function of these cells. An alternative explanation, which is supported by the large increase in Hθ reported by Venner and colleagues after CNO dosing (31), is that the increase in Wake is a secondary consequence of the LMA increase, thereby challenging the notion that LH inhibitory neurons are involved in sleep/wake regulation.

Future studies will focus on the identification of even more specific molecular markers of these glutamatergic wake-promoting neurons than CaMKIIα, as well as the inputs to these cells. Loss of function experiments will be critical to determine whether

suppression of these neurons reproduces the lethargy observed in the classic studies of von Economo (10) and whether these neurons are indeed the key that has been missing for nearly a century to explain how LH contributes to the regulation of sleep and wakefulness.

Perspective. The prolonged wakefulness duration produced by LH CaMKIIα neuron activation even in the absence of Hcrt signaling (Fig. 1*B*) suggests a possible therapeutic path for treatment of one of the primary symptoms of the sleep disorder narcolepsy: the inability to sustain wakefulness for an extended period of time. Activating this wake-promoting population might mitigate the symptoms of narcolepsy and other disorders of excessive daytime sleepiness. Thus, the identification of distinct LH neuronal populations that regulate wakefulness and LMA may influence the development of new therapies to treat sleep-related disorders as well as other neurological and psychiatric diseases.

Materials and Methods

Animals. Male and female C57BL/6J (RRID:IMSR_JAX:000664), *Vglut2-IRES-Cre* (RRID:IMSR_JAX:016963), *Gad2-IRES-Cre* (RRID:IMSR_JAX:010802) and R26R-EYFP reporter (RRID:IMSR_JAX:006148) mice were obtained from Jackson Laboratory and subsequently bred at SRI International. Mice were housed in standard polycarbonate cages at a constant temperature (24 ± 2 °C) and humidity (50 ± 20% relative humidity) with food and water *ad libitum* under a 12 h:12 h light–dark cycle, with dim red lights (<2 lx) kept on at all times to facilitate handling mice during the dark phase. Experiments were performed on adult mice (>8 wk) of both sexes. All studies were conducted in accordance with the Guide for the Care and Use of Laboratory Animals and were approved by the Institutional Animal Care and Use Committee at SRI International. Every effort was made to minimize animal discomfort throughout these studies.

Surgical Procedures. See *SI Appendix*

EEG/EMG Recording. To allow acclimation to the recording apparatus, mice were connected to a tether that was attached to a commutator (Pinnacle Technology, Inc.) for at least 5 d before experiments. The commutator allowed the mice to move freely in their home cages. For acclimation to the dosing procedure, mice underwent three intraperitoneal injections of saline (SAL) on different days before initiation of the dosing studies. Experiments occurred no sooner than 21 d after the EEG/EMG implantation surgery. EEG and EMG data were collected at 800 Hz and digitally band passed at 0.5 to 300 Hz using a TDT RZ2 system connected to a 96-channel PZ2 amplifier and a low impedance RA16LI-D headstage (Tucker-Davis Technologies). All mice underwent an undisturbed 24-h baseline recording in their home cages before dosing experiments.

Dosing Procedure. For chemogenetic experiments in *Vglut2-IRES-Cre* mice (*SI Appendix*, Fig. S1), the hM3Dq ligand deschloroclozapine (DCZ; Hello bio #: HB8555) was injected at 0.3 mg/kg, i.p., in physiological SAL at a concentration of 0.03 mg/mL. For the CaMKIIα chemogenetic experiments in WT mice, the hM3Dq ligand CNO (catalog #4936, Tocris Bioscience) was injected 3 mg/kg, i.p. in SAL at a concentration of 0.5 mg/mL. To block Hcrt signaling, the dual orexin receptor antagonist ALM, synthesized at SRI International (53), was injected intraperitoneally at a concentration of 200 mg/kg in VEH consisting of 1.25% hydroxypropyl methyl cellulose (SKU 09963), 0.1% dioctyl sodium sulfosuccinate (SKU 323586), and 0.25% methyl cellulose (SKU 274429) in water (all from Sigma-Aldrich) after vortexing a 30 mg/mL solution for 2 h. Dosing sessions were at least 4 d apart and at least 7 d elapsed between CNO dosings. Recordings started 1 h prior to dosing and lasted until ZT12.

Calcium Imaging. At least 2 wk after lens and EEG/EMG electrode implantation, mice were briefly restrained for attachment and focusing of the microscope, returned to their home cage which was placed in a recording chamber, and then allowed at least 1h for recovery from handling before recording began. Around ZT3–ZT5, concurrent recording of EEG/EMG and Ca^{2+} imaging at 15 fps using an nVista microendoscope (Inscopix, Palo Alto, CA) was initiated. Recording sessions lasted for 120 min during which 2 min imaging periods were interspersed with 30 s "rest periods" to prevent overheating of tissue due to prolonged exposure to light during imaging. To synchronize the EEG and video recordings, a TTL signal pulse was recorded together with the EEG traces every time a frame was acquired by nVista.

Analysis of Calcium Imaging Data. See *SI Appendix*

LMA Data Collection and Analysis. Locomotion was monitored by a Vium Smart Housing system (Vium, Inc., San Mateo, CA) which continuously records and streams the respiratory rate and locomotion of free-moving mice in their home cage (67). Locomotion was exported as a .csv file in 10 min bins and processed with custom scripts in Python.

EEG/EMG Data Collection and Analysis. Using the criteria described previously (36, 68, 69), EEG/EMG data were visually scored as wake (W), NREM, or REM in 4-s epochs. A bout of W, NREM, or REM was defined as two consecutive 4-s epochs (i.e., 8 s) within the same state. This minimal bout duration was chosen to allow for a finer resolution of bout durations. For quantitative EEG analysis, the power spectrum was calculated for each 4-s artifact-free epoch using the squared amplitude coefficients of the fast Fourier transform and the mean power in the delta (δ), 0.5 to 4 Hz; low theta (Lθ), 4 to 8 Hz; high theta (Hθ), 8 to 10 Hz; low gamma (Lγ), 15 to 50 Hz; high gamma (Hγ), 60 to 80 Hz; and very high gamma (Vhγ), 90 to 200 Hz. To avoid the 60-Hz artifact, the spectral power values at 60 ± 1 Hz and the harmonics at 120 and 180 Hz were replaced by a linear interpolation from the values at 59 and 61, 119 and 121, and 179 and 181 Hz. Normalized Wake power was obtained by dividing the mean power spectrum during Wake by the mean power in Wake during the same time period of a baseline recording.

Histology and Cell Counting Procedures. See *SI Appendix*.

Statistics. Results obtained from male mice were similar to those of female mice and thus data from both sexes were grouped. For statistical analysis, we performed two-way RM-ANOVA using Sigmaplot (Systat Software Inc.) followed by Bonferroni-corrected *post hoc t* tests to identify effects of the different treatments on sleep architecture across time after dosing. For comparisons involving only one factor, we used the MATLAB function anova1 followed by Tukey's *post hoc* test with Bonferroni correction to identify individual differences between two treatments. To compare the effect of two factors on two different populations, we performed an unbalanced two-way ANOVA using the MATLAB function anovan. For estimation of whether two datasets had the same probability distribution, we used the two-sample Kolmogorov–Smirnov goodness-of-fit hypothesis test with the MATLAB function kstest2. The Bonferroni correction was also used here for pairwise comparison of more than two distributions.

Data, Materials, and Software Availability. The data underlying the present work will be available on the National Sleep Research Resource (70) website (https://sleepdata.org). Matlab and Python code will be available at https://github.com/.

ACKNOWLEDGMENTS. Research supported by R01NS077408 and R01NS098813 from the NIH to T.S.K. and by KAKENHI grants 18H05124, 18KK0223, and 18H02523 to A.Y. from the Ministry of Education, Culture, Sports Science, MEXT, Japan. The content is solely the responsibility of the authors and does not necessarily represent the official views of the NIH. We thank Inscopix customer support for their assistance with microendoscopic imaging.

Author affiliations: [a]Center for Neuroscience, Biosciences Division, SRI International, Menlo Park, CA 94025; and [b]Department of Neuroscience II, Research Institute of Environmental Medicine, Nagoya University, Nagoya 464-8601, Japan

1. P. Bonnavion, L. E. Mickelsen, A. Fujita, L. de Lecea, A. C. Jackson, Hubs and spokes of the lateral hypothalamus: Cell types, circuits and behaviour. *J. Physiol.* **594**, 6443–6462 (2016).
2. L. E. Mickelsen *et al.*, Single-cell transcriptomic analysis of the lateral hypothalamic area reveals molecularly distinct populations of inhibitory and excitatory neurons. *Nat. Neurosci.* **22**, 642–656 (2019).
3. L. Steuernagel *et al.*, HypoMap-a unified single-cell gene expression atlas of the murine hypothalamus. *Nat. Metab.* **4**, 1402–1419 (2022).
4. H. Fong, J. Zheng, D. Kurrasch, The structural and functional complexity of the integrative hypothalamus. *Science* **382**, 388–394 (2023).

5. A. C. Jackson, A common framework for mouse hypothalamic cell atlases. *Nat. Metab.* **4**, 1227–1228 (2022).
6. G. D. Stuber, Neurocircuits for motivation. *Science* **382**, 394–398 (2023).
7. L. Mei, T. Osakada, D. Lin, Hypothalamic control of innate social behaviors. *Science* **382**, 399–404 (2023).
8. P. H. Luppi, P. Fort, Sleep–wake physiology. *Handb. Clin. Neurol.* **160**, 359–370 (2019).
9. A. R. Adamantidis, L. de Lecea, Sleep and the hypothalamus. *Science* **382**, 405–412 (2023).
10. C. von Economo, Sleep as a problem of localization. *J. Nerv. Ment. Dis.* **71**, 249–259 (1930).
11. S. W. Ranson, Somnolence caused by hypothalamic lesions in the monkey. *Arch. Neurol. Psychiat.* **41**, 1–23 (1939).
12. W. J. H. Nauta, Hypothalamic regulation of sleep in rats. An experimental study. *J. Neurophysiol.* **9**, 285–316 (1946).
13. M. de Ryck, P. Teitelbaum, Neocortical and hippocampal EEG in normal and lateral hypothalamic-damaged rats. *Physiol. Behav.* **20**, 403–409 (1978).
14. S. Shoham, P. Teitelbaum, Subcortical waking and sleep during lateral hypothalamic "somnolence" in rats. *Physiol. Behav.* **28**, 323–333 (1982).
15. M. Cerri *et al.*, Enhanced slow-wave EEG activity and thermoregulatory impairment following the inhibition of the lateral hypothalamus in the rat. *PLoS One* **9**, e112849 (2014).
16. L. Krolicki, A. Chodobski, K. Skolasinska, The effect of stimulation of the reticulo-hypothalamic-hippocampal systems on the cerebral blood flow and neocortical and hippocampal electrical activity in cats. *Exp. Brain Res.* **60**, 551–558 (1985).
17. H. M. Sinnamon, M. E. Karvosky, C. P. Ilch, Locomotion and head scanning initiated by hypothalamic stimulation are inversely related. *Behav. Brain Res.* **99**, 219–229 (1999).
18. M. A. Alam, B. N. Mallick, Glutamic acid stimulation of the perifornical–lateral hypothalamic area promotes arousal and inhibits non-REM/REM sleep. *Neurosci. Lett.* **439**, 281–286 (2008).
19. F. W. Li, S. Deurveilher, K. Semba, Behavioural and neuronal activation after microinjections of AMPA and NMDA into the perifornical lateral hypothalamus in rats. *Behav. Brain Res.* **224**, 376–386 (2011).
20. M. N. Alam *et al.*, Sleep-waking discharge patterns of neurons recorded in the rat perifornical lateral hypothalamic area. *J. Physiol.* **538**, 619–631 (2002).
21. Y. Koyama, K. Takahashi, T. Kodama, Y. Kayama, State-dependent activity of neurons in the perifornical hypothalamic area during sleep and waking. *Neuroscience* **119**, 1209–1219 (2003).
22. M. G. Lee, O. K. Hassani, B. E. Jones, Discharge of identified orexin/hypocretin neurons across the sleep-waking cycle. *J. Neurosci.* **25**, 6716–6720 (2005).
23. L. de Lecea *et al.*, The hypocretins: Hypothalamus-specific peptides with neuroexcitatory activity. *Proc. Natl. Acad. Sci. U.S.A.* **95**, 322–327 (1998).
24. T. Sakurai *et al.*, Orexins and orexin receptors: A family of hypothalamic neuropeptides and G protein-coupled receptors that regulate feeding behavior. *Cell* **92**, 573–585 (1998).
25. C. Peyron *et al.*, Neurons containing hypocretin (orexin) project to multiple neuronal systems. *J. Neurosci.* **18**, 9996–10015 (1998).
26. F. Torrealba, M. Yanagisawa, C. B. Saper, Colocalization of orexin a and glutamate immunoreactivity in axon terminals in the tuberomammillary nucleus in rats. *Neuroscience* **119**, 1033–1044 (2003).
27. K. S. Eriksson, O. A. Sergeeva, O. Selbach, H. L. Haas, Orexin (hypocretin)/dynorphin neurons control GABAergic inputs to tuberomammillary neurons. *Eur. J. Neurosci.* **19**, 1278–1284 (2004).
28. C. Schone *et al.*, Optogenetic probing of fast glutamatergic transmission from hypocretin/orexin to histamine neurons in situ. *J. Neurosci.* **32**, 12437–12443 (2012).
29. C. Schone, J. Apergis-Schoute, T. Sakurai, A. Adamantidis, D. Burdakov, Coreleased orexin and glutamate evoke nonredundant spike outputs and computations in histamine neurons. *Cell Rep.* **7**, 697–704 (2014).
30. C. B. Saper, T. E. Scammell, J. Lu, Hypothalamic regulation of sleep and circadian rhythms. *Nature* **437**, 1257–1263 (2005).
31. A. Venner, C. Anaclet, R. Y. Broadhurst, C. B. Saper, P. M. Fuller, A novel population of wake-promoting GABAergic neurons in the ventral lateral hypothalamus. *Curr. Biol.* **26**, 2137–2143 (2016).
32. C. G. Herrera *et al.*, Hypothalamic feedforward inhibition of thalamocortical network controls arousal and consciousness. *Nat. Neurosci.* **19**, 290–298 (2016).
33. F. Naganuma *et al.*, Lateral hypothalamic neurotensin neurons promote arousal and hyperthermia. *PLoS Biol.* **17**, e3000172 (2019).
34. N. P. Pedersen *et al.*, Supramammillary glutamate neurons are a key node of the arousal system. *Nat. Commun.* **8**, 1405 (2017).
35. R. F. Wang *et al.*, Control of wakefulness by lateral hypothalamic glutamatergic neurons in male mice. *J. Neurosci. Res.* **99**, 1689–1703 (2021).
36. J. E. Heiss, A. Yamanaka, T. S. Kilduff, Parallel arousal pathways in the lateral hypothalamus. *eNeuro* **5**, 0228–0318 (2018).
37. C. Perez-Leighton, M. R. Little, M. Grace, C. Billington, C. M. Kotz, Orexin signaling in rostral lateral hypothalamus and nucleus accumbens shell in the control of spontaneous physical activity in high- and low-activity rats. *Am. J. Physiol. Regul. Integr. Comp. Physiol.* **312**, R338–R346 (2017).
38. C. Kosse, C. Schone, E. Bracey, D. Burdakov, Orexin-driven GAD65 network of the lateral hypothalamus sets physical activity in mice. *Proc. Natl. Acad. Sci. U.S.A.* **114**, 4525–4530 (2017).
39. E. Qualls-Creekmore *et al.*, Galanin-expressing GABA neurons in the lateral hypothalamus modulate food reward and noncompulsive locomotion. *J. Neurosci.* **37**, 6053–6065 (2017).
40. J. S. Farrell *et al.*, Supramammillary regulation of locomotion and hippocampal activity. *Science* **374**, 1492–1496 (2021).
41. T. S. Kilduff, C. Peyron, The hypocretin/orexin ligand-receptor system: Implications for sleep and sleep disorders. *Trends Neurosci.* **23**, 359–365 (2000).
42. C. Peyron *et al.*, A mutation in a case of early onset narcolepsy and a generalized absence of hypocretin peptides in human narcoleptic brains. *Nat. Med.* **6**, 991–997 (2000).
43. T. Thannickal *et al.*, Reduced number of hypocretin neurons in human narcolepsy. *Neuron* **27**, 469–474 (2000).
44. T. S. Kilduff, The mystery of GHB efficacy in narcolepsy type 1. *Sleep* **46**, zsad156 (2023), 10.1093/sleep/zsad156.
45. X. B. Liu, E. G. Jones, Localization of alpha type II calcium calmodulin-dependent protein kinase at glutamatergic but not gamma-aminobutyric acid (GABAergic) synapses in thalamus and cerebral cortex. *Proc. Natl. Acad. Sci. U.S.A.* **93**, 7332–7336 (1996).
46. A. Sik, N. Hajos, A. Gulacsi, I. Mody, T. F. Freund, The absence of a major Ca2+ signaling pathway in GABAergic neurons of the hippocampus. *Proc. Natl. Acad. Sci. U.S.A.* **95**, 3245–3250 (1998).
47. X. Wang, C. Zhang, G. Szabo, Q. Q. Sun, Distribution of CaMKIIalpha expression in the brain in vivo, studied by CaMKIIalpha-GFP mice. *Brain Res.* **1518**, 9–25 (2013).
48. Y. Nagai *et al.*, Deschloroclozapine, a potent and selective chemogenetic actuator enables rapid neuronal and behavioral modulations in mice and monkeys. *Nat. Neurosci.* **23**, 1157–1167 (2020).
49. S. Zhang *et al.*, Molecular basis for selective activation of DREADD-based chemogenetics. *Nature* **612**, 354–362 (2022).
50. G. Buzsaki, E. I. Moser, Memory, navigation and theta rhythm in the hippocampal-entorhinal system. *Nat. Neurosci.* **16**, 130–138 (2013).
51. G. Buzsaki, Theta oscillations in the hippocampus. *Neuron* **33**, 325–340 (2002).
52. C. H. Vanderwolf, Hippocampal electrical activity and voluntary movement in the rat. *Electroencephalogr. Clin. Neurophysiol.* **26**, 407–418 (1969).
53. S. W. Black *et al.*, Almorexant promotes sleep and exacerbates cataplexy in a murine model of narcolepsy. *Sleep* **36**, 325–336 (2013).
54. J. L. Gomez *et al.*, Chemogenetics revealed: DREADD occupancy and activation via converted clozapine. *Science* **357**, 503–507 (2017).
55. K. S. Chen *et al.*, A hypothalamic switch for REM and non-REM sleep. *Neuron* **97**, 1168–1176.e4 (2018).
56. K. K. Ghosh *et al.*, Miniaturized integration of a fluorescence microscope. *Nat. Methods* **8**, 871–878 (2011).
57. H. Taniguchi *et al.*, A resource of Cre driver lines for genetic targeting of GABAergic neurons in cerebral cortex. *Neuron* **71**, 995–1013 (2011).
58. K. Sasaki *et al.*, Pharmacogenetic modulation of orexin neurons alters sleep/wakefulness states in mice. *PLoS One* **6**, e20360 (2011).
59. A. R. Adamantidis, F. Zhang, A. M. Aravanis, K. Deisseroth, L. de Lecea, Neural substrates of awakening probed with optogenetic control of hypocretin neurons. *Nature* **450**, 420–424 (2007).
60. J. M. Veres, T. Andrasi, P. Nagy-Pal, N. Hajos, CaMKIIalpha promoter-controlled circuit manipulations target both pyramidal cells and inhibitory interneurons in cortical networks. *eNeuro* **10** (2023).
61. X. He *et al.*, Gating of hippocampal rhythms and memory by synaptic plasticity in inhibitory interneurons. *Neuron* **109**, 1013–1028.e9 (2021).
62. N. Moragues, P. Ciofi, P. Lafon, G. Tramu, M. Garret, GABAA receptor epsilon subunit expression in identified peptidergic neurons of the rat hypothalamus. *Brain Res.* **967**, 285–289 (2003).
63. C. F. Elias *et al.*, Characterization of CART neurons in the rat and human hypothalamus. *J. Comp. Neurol.* **432**, 1–19 (2001).
64. L. E. Mickelsen *et al.*, Neurochemical heterogeneity among lateral hypothalamic hypocretin/orexin and melanin-concentrating hormone neurons identified through single-cell gene expression analysis. *eNeuro* **4**, 0013–0017 (2017).
65. M. J. Chee, E. Arrigoni, E. Maratos-Flier, Melanin-concentrating hormone neurons release glutamate for feedforward inhibition of the lateral septum. *J. Neurosci.* **35**, 3644–3651 (2015).
66. M. Schneeberger *et al.*, Functional analysis reveals differential effects of glutamate and MCH neuropeptide in MCH neurons. *Mol. Metab.* **13**, 83–89 (2018).
67. S. W. Baran *et al.*, Digital biomarkers enable automated, longitudinal monitoring in a mouse model of aging. *J. Gerontol. A Biol. Sci. Med. Sci.* **76**, 1206–1213 (2021).
68. L. Dittrich, S. R. Morairty, D. R. Warrier, T. S. Kilduff, Homeostatic sleep pressure is the primary factor for activation of cortical nNOS/NK1 neurons. *Neuropsychopharmacology* **40**, 632–639 (2015).
69. S. R. Morairty *et al.*, A role for cortical nNOS/NK1 neurons in coupling homeostatic sleep drive to EEG slow wave activity. *Proc. Natl. Acad. Sci. U.S.A.* **110**, 20272–20277 (2013).
70. G. Q. Zhang *et al.*, The National Sleep Research Resource: Towards a sleep data commons. *J. Am. Med. Inform. Assoc.* **25**, 1351–1358 (2018).